

AD-A043 126

TEXAS TECH UNIV LUBBOCK DEPT OF ELECTRICAL ENGINEERING F/G 20/2
SECOND BREAKDOWN BEHAVIOR OF A SINGLE MICROPLASMA P-N JUNCTION.(U)
AUG 76 W M PORTNOY, L J STOTTS DAAG39-74-C-0054

UNCLASSIFIED

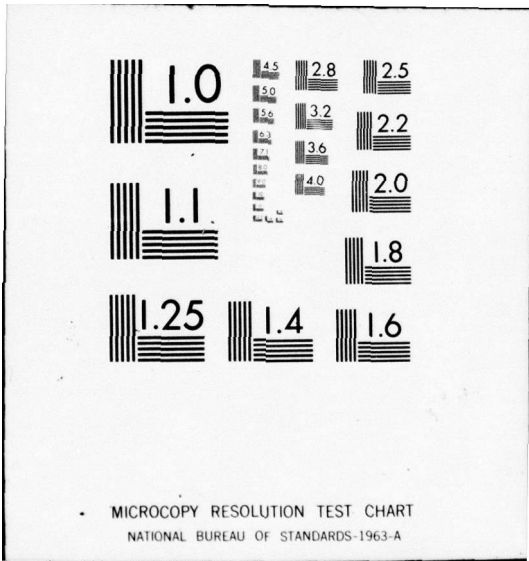
HDL-CR-76-054-1

NL

1 of 1
ADA043126



END
DATE
FILMED
9-77
DDC



HDL-CR-76-064-1

⑧ J

ADA043126

SECOND BREAKDOWN BEHAVIOR OF A SINGLE MICROPLASMA p-n JUNCTION

CR-76-064-1—Second Breakdown Behavior of a Single Microplasma p-n Junction—
by William M. Portnoy and Larry J. Stotts

AUGUST 1976

Prepared by

Integrated and Hybrid Circuits Laboratory
Department of Electrical Engineering
Texas Tech University
Lubbock, Texas 79409

Under Contract
DAAG 39-74-C-0054

DDC
RECEIVED
AUG 22 1977
A



AD NO
DDC FILE COPY

U.S. Army Materiel Development
and Readiness Command
HARRY DIAMOND LABORATORIES
Adelphi, Maryland 20783

The findings in this report are not to be construed as an official Department of the Army position unless so designated by other authorized documents.

Citation of manufacturers' or trade names does not constitute an official endorsement or approval of the use thereof.

Destroy this report when it is no longer needed. Do not return it to the originator.

ACCESSION for	
NTIS	White Section <input checked="" type="checkbox"/>
DDC	Buff Section <input type="checkbox"/>
UNANNOUNCED JUSTIFICATION	<input type="checkbox"/>
BY	
DISTRIBUTION/AVAILABILITY CODES	
Dist.	AVAIL. AND/OR SPECIAL
A	

UNCLASSIFIED

SECURITY CLASSIFICATION OF THIS PAGE (When Data Entered)

19 REPORT DOCUMENTATION PAGE		READ INSTRUCTIONS BEFORE COMPLETING FORM	
1. REPORT NUMBER 18 HDL-CR-76-054-1	2. JOVT ACCESSION NO.	3. RECIPIENT'S CATALOG NUMBER 9	
4. TITLE (and Subtitle) 6 Second Breakdown Behavior of a Single Microplasma p-n Junction		5. TYPE OF REPORT & PERIOD COVERED Contractor's Report	
7. AUTHOR(s) 10 William M./Portnoy Larry J./Stotts		8. CONTRACT OR GRANT NUMBER(s) 15 DAAG 39-74-C-0054	
9. PERFORMING ORGANIZATION NAME AND ADDRESS Department of Electrical Engineering Texas Tech University Lubbock, Texas 79409		10. PROGRAM ELEMENT, PROJECT, TASK AREA & WORK UNIT NUMBERS Program: 6.21.18.A 16 DA: 1W162118AD51	
11. CONTROLLING OFFICE NAME AND ADDRESS Harry Diamond Laboratories 2800 Powder Mill Road Adelphi, Md. 20783		12. REPORT DATE 11 August 1976	
14. MONITORING AGENCY NAME & ADDRESS (if different from Controlling Office) 12 36p.		13. NUMBER OF PAGES 39	
		15. SECURITY CLASS. (of this report) UNCLASSIFIED	
		15a. DECLASSIFICATION/DOWNGRADING SCHEDULE	
16. DISTRIBUTION STATEMENT (of this Report) Approved for public release; distribution unlimited.			
17. DISTRIBUTION STATEMENT (of the abstract entered in Block 20, if different from Report)			
18. SUPPLEMENTARY NOTES HDL Project: X514E1 DRCMS Code: 612118.11.D5100			
19. KEY WORDS (Continue on reverse side if necessary and identify by block number) Second breakdown Junction temperature Pulsed measurements Electrothermal instability			
20. ABSTRACT (Continue on reverse side if necessary and identify by block number) This report describes the results of pulsed measurements of the voltage across a p-n junction. The junction was formed by alloying aluminum into n-type silicon to form a pyramidal structure, the apex being the breakdown site. Voltages at second breakdown were related to junction temperature by way of the temperature dependence of the avalanche breakdown voltage. The temperature measurements support a thermal runaway mechanism for second breakdown.			

CONTENTS

	<u>Page</u>
1. INTRODUCTION.	5
2. THEORY OF THE MEASUREMENTS.	10
2.1 Double-Pulse Technique	11
2.2 Single-Pulse Technique	12
3. DIODE FABRICATION	16
4. MEASUREMENTS AND RESULTS.	19
4.1 Temperature Coefficient of Avalanche Break- down Voltage	20
4.2 Junction Temperature at Second Breakdown	20
5. DISCUSSION OF RESULTS	23
6. LITERATURE CITED.	31
7. SELECTED BIBLIOGRAPHY	32
8. DISTRIBUTION.	37

FIGURES

1	Characteristic curve for a p-n junction diode showing the transition into second breakdown	7
2	Junction voltage and current pulses in second breakdown.	8
3	Effects of temperature on junction diode characteristics.	13
4	Circuit for temperature dependent voltage measurements.	14
5	Voltage and current waveforms for the double-pulse measurement.	17
6	Voltage and current waveforms for the single-pulse measurement.	18

CONTENTS (Continued)

	<u>Page</u>
7	Pyramidal junction configuration. 21
8	Measured diode characteristic curves. 22
9	Junction reverse voltage waveforms with constant current pulses. 25
10	Events in second breakdown: junction reverse voltage with a constant current pulse 28
11	Junction reverse voltage <i>vs.</i> time: current nucleation. 29
12	Resistivity-temperature curves for silicon. . . . 30
	Table I. Summary of Temperature Measurements . . 26

1. INTRODUCTION

Second breakdown is a form of electrothermal instability in p-n junction devices which is characterized by a sudden, often discontinuous, drop in the voltage across the device with a simultaneous increase in current through the device (figure 1). This phenomenon in semiconductor junctions has been intensively studied in the past decade, with the various theories having as their common basis the formation of current nonuniformities which can carry a localized portion of the device into operating regions where second breakdown occurs. Schafft¹ has published an excellent review of the work done on second breakdown up to 1967, and the majority of the work seems to indicate that second breakdown is thermal in origin. This conclusion was, in part, based on thermal studies at the surface of p-n junction devices using heat sensitive emulsions, whose transmittance varied in response to local temperature changes. This method, however, is too slow to provide any clues to the order of events which take place when second breakdown occurs.

Second breakdown usually results in degradation of device characteristics; however, it need not be destructive, and it has been studied using short, controlled current pulses at low repetition rates. Figure 2 shows a voltage-current-time characterization of second breakdown when a voltage pulse is applied. In most devices, second breakdown does not take place instantaneously, but only after the device has been at the operating point for a certain period of time called the delay time. The delay time has been found to vary inversely with voltage for a given current, indicating an energy dependence in the breakdown mechanism. These results have supported the concept of a minimum critical energy, rather than a critical temperature, which causes the transition into second breakdown, and a thermal mechanism for second breakdown.

More recent studies have coupled thermal resistance measurements with optical observations to demonstrate the importance of current filamentation in the second

¹H. A. Shaft, *Second Breakdown - A Comprehensive Review*, Proc. IEEE, 55 (1967), 1272.

breakdown process. Current filamentation is a nonlinear phenomenon in which conductance in a region switches from near uniformity to a state in which the conductance of a particular filament greatly exceeds that of the surrounding material. The initiation of these non-uniformities has been ascribed to debiasing effects, lateral thermal instabilities, and space-charge effects resulting from high densities of free charged carriers.^{1,2} The latter nonthermal effect normally involves a concentration gradient that arises from the junction configuration. However, second breakdown has been shown to be a very general phenomenon, not one that is unique to specific geometries.³

The most acute problem in studying second breakdown is in obtaining a clear picture of the order in which various events take place. Current filaments are usually buried deep within the sample, so that a time correlation between optical, thermal, and electrical measurement is very difficult. In the past several years, a stroboscopic technique^{4,5,6} has been used on thin film SOS diodes. This technique employs the change with temperature of the optical transmittance of visible light through thin silicon films (less than one micron) as a real time temperature sensor; a series of pictures can be obtained which are time correlated with the voltage and current waveforms.

¹H. A. Schafft, *Second Breakdown - A Comprehensive Review*, Proc. IEEE, 55 (1967), 1272.

²H. Potash and W. W. Happ, *Modeling Procedures for Interactions Between Thermal and Electrical Device Parameters*, Solid-St. Electr., 10 (1967), 737.

³P. P. Budenstein, D. H. Pontius and W. B. Smith, *Second Breakdown Damage in Semiconductor Junction Devices*, US Army Missile Command, Redstone Arsenal, Report RA-TR-72-15 (1972).

⁴P. P. Budenstein, *A Survey of Second Breakdown Phenomena, Mechanisms, and Damage in Semiconductor Devices*, Defense Documentation Center Report AD-721294 (1970).

⁵R. Sunshine, *Avalanching and Second Breakdown in Silicon-on-Sapphire Diodes*, Ph.D. Dissertation, Princeton University (1971).

⁶W. B. Smith, D. H. Pontius and P. P. Budenstein, *Second Breakdown and Damage in Junction Devices*, IEEE Trans. El. Dev., ED-20 (1973), 731.

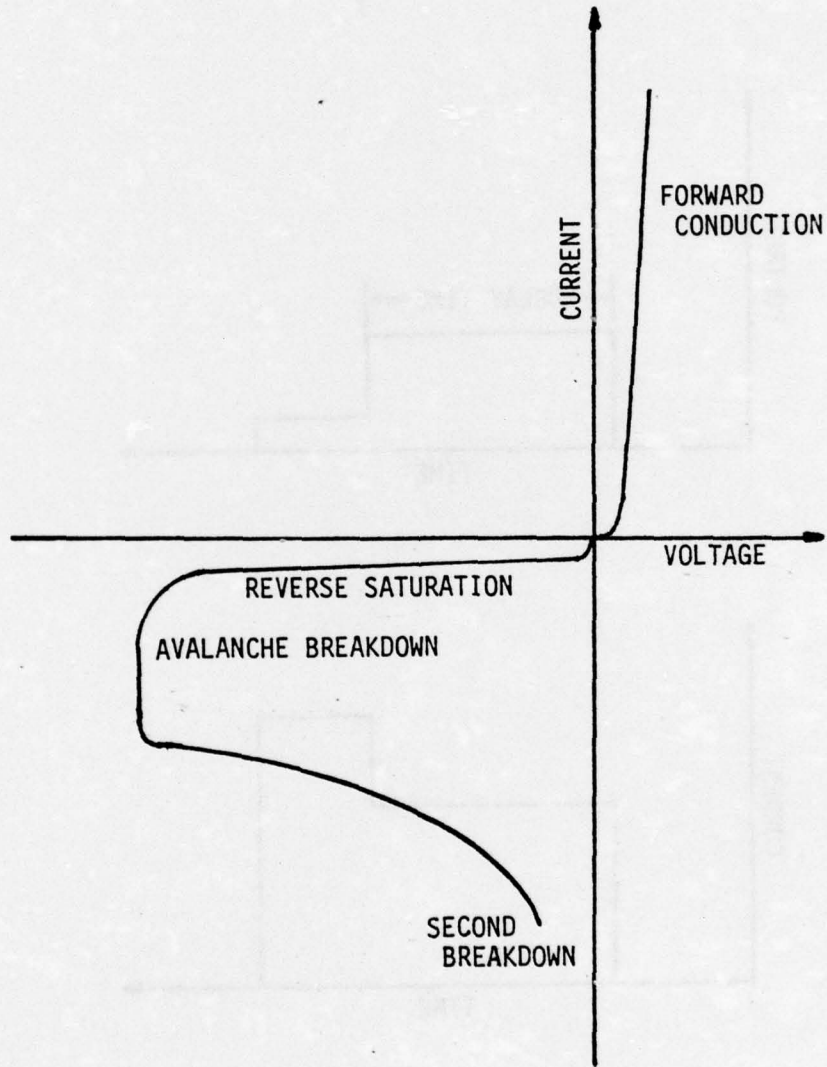


Figure 1. Characteristic curve for a p-n junction diode showing the transition into second breakdown.

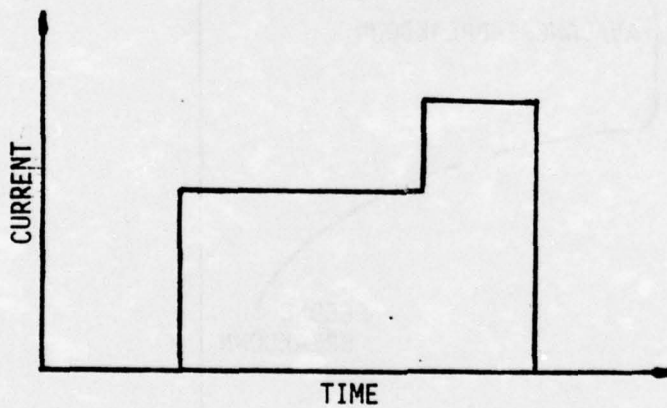
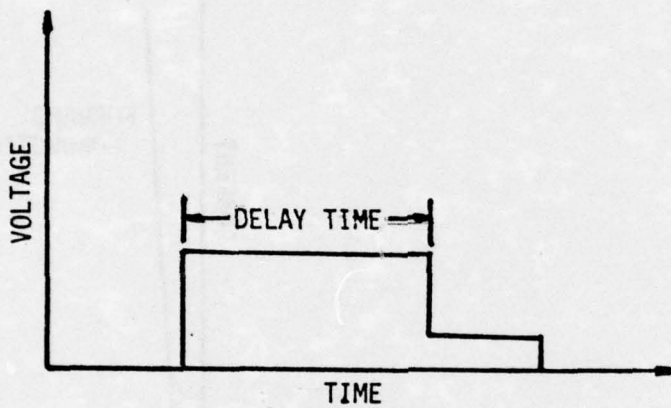


Figure 2. Junction voltage and current pulses in second breakdown.

The pictorial sequence is then related to the order of events in second breakdown. However, because of the highly specific type of the junction devices used, it is difficult to generalize the results. Nonetheless, this work has associated heretofore unnoticed characteristics of the voltage waveform in constant current pulsing with the occurrence of definite physical events. For example, a subtle fluctuation in the voltage waveform was found to be coincident with the nucleation of small current channels. This is an important event in many theories of second breakdown, but it has never been specifically linked to any observations of the voltage waveform. These results will be discussed in greater detail below.

The physical phenomena associated with second breakdown (current channeling and so on) can take place at different locations within the junction region during any single transition into second breakdown. The breakdown sites usually occur in reproducible configurations for a given input power, and no satisfactory explanation has yet been given for this behavior. These sites may be a characteristic of heat flow for a particular junction geometry, or microplasmas which occur during avalanche breakdown may become locations for second breakdown if current is sufficiently localized. Although it has been demonstrated that line defects have no effect on second breakdown,¹ microplasmas may occur at point defects, which are not detectible by x-ray analysis, and inasmuch as a microplasma initiation mechanism may be important, second breakdown could occur at sites which provide no observable correlation with structural defects.

In the work described here, the second breakdown characteristics of a single identifiable breakdown site were studied by fabricating a p-n junction such that microplasma formation would occur substantially only at one location. Aluminum was alloyed into the (100) surface of a slice of n-type silicon such that the breakdown character of the diode structure was dominated by the microplasma formed at the apex of the resulting pyramidal junc-

¹H. A. Schaft, *Second Breakdown - A Comprehensive Review*, Proc. IEEE, 55 (1967), 1272.

tion. The pulse techniques of Chiang and Lauritzen⁷ and Nigrin⁸ were used to determine the internal temperature of the junction just before the onset of second breakdown. The voltage waveform produced by constant current pulsing was examined using a differential voltage comparator; this measurement was an improvement over previous ones because, by floating the voltage waveform in a precise manner, important features riding on top of the waveform could be observed on a more sensitive scale. An additional improvement over previous work was the recording of fast waveform events with a storage oscilloscope.

This report contains a discussion of the theory of pulsed temperature measurements, and a description of the construction of the pyramidal shaped junction. The results of the measurements are presented and discussed, and related to the results of other work, as well as to second breakdown in general. The report is supplemented by a bibliography containing references to important second breakdown studies performed since 1967.

2. THEORY OF THE MEASUREMENTS

In order to identify the mechanism that triggers second breakdown, an accurate junction temperature measurement must be obtained at the breakdown threshold. Temperature sensitive parameters of a p-n junction are the best indicators of average junction temperature. Some of these are the voltage drop across a forward biased junction at constant current, the junction avalanche breakdown voltage, and the saturation current of a reverse-biased junction at constant voltage. Figure 3 illustrates the change with temperature in the shape of the characteristic curve for a junction diode. The changes which are shown with increasing temperature are an increase in reverse saturation current, an increase in forward conduction current, a decrease in reverse incremental resistance, and an increase in the avalanche breakdown voltage. The last of these was used here to determine average junction temperature just

⁷K. L. Chiang and P. O. Lauritzen, *Thermal Instability in Very Small p-n Junction*, *IEEE Trans. El. Dev.*, *ED-17* (1970), 782.

⁸J. Nigrin, *Pulse Measurements of Transient Thermal Response and Temperature of Avalanching p-n Junction*, *Electr. Letters*, *1* (1971), 481.

prior to the onset of second breakdown, employing two pulse techniques for sampling the breakdown voltage.

2.1 Double-Pulse Technique

This method is based on a technique first used by Nigrin⁸ for studying avalanche voltage transients. In the original measurement, the diode was driven into avalanche with a biasing pulse, and the instantaneous junction breakdown voltage was sampled by a fast pulse of such polarity and amplitude that the diode current at the pulse leading edge was essentially zero. If the pulse risetime is fast, there will be no heating on the leading edge, and the sampled value at the leading edge will correspond to conditions preceding the pulse. The measured value is compared with the breakdown voltage obtained with a similar sampling pulse at a known constant ambient temperature to obtain the junction temperature. The actual junction temperature, T_J , is higher than the measured temperature, T_{Jm} , because of the non-zero power dissipation at the junction during the measurement. The actual junction temperature can be calculated from the measured junction temperature if the heat flow resistance between the diode and heat sink, θ , is known:

$$T_J = T_{Jm} + \theta V_B(T_{Jm}) I_B \quad (1)$$

where $V_B(T_{Jm})$ is the instantaneous avalanche breakdown voltage, and I_B is the value of the diode reverse current at avalanche breakdown. The heat flow resistance is found by making temperature measurements at two input power levels and assuming that θ does not change significantly with temperature for small temperature increments. Then

$$\theta = \frac{\Delta T}{\Delta P} = \frac{T_{Jm2} - T_{Jm1}}{V_2 I_2 - V_1 I_1} \quad (2)$$

To measure the junction temperature preceding second breakdown, a pair of pulse generators are used in the con-

⁸J. Nigrin, *Pulse Measurements of Transient Thermal Response and Temperature of Avalanche p-n Junction*, *Electr. Letters*, 1 (1971), 481.

figuration of figure 4. A low value of the diode reverse current, I_B , is chosen to define the avalanche breakdown voltage. The voltage applied to the diode consists of a short sampling pulse superimposed on a longer bias pulse which drives the diode into second breakdown. Their repetition rates and widths are low enough so that they do not affect the average thermal conditions of the junction. The sampling pulse polarity is such that the diode voltage is reduced towards the instantaneous breakdown voltage, $V_B(T_{Jm})$, just before the onset of second breakdown. If the amplitude of the sampling pulse is so adjusted that the current at the pulse leading edge is just the current level defining avalanche, then the differential voltage across the diode will be $V_B(T_{Jm})$ (figure 5), where T_{Jm} is now the measured junction temperature just prior to second breakdown.

2.2 Single-Pulse Technique

When a p-n junction diode is biased into avalanche breakdown, the avalanche current, I_B , is determined by the diode spreading resistance, R_{SP} , the space charge resistance, R_{SC} , and the magnitude of the applied voltage, V , above the breakdown voltage, V_B :

$$V - V_B(T_J) = I_B(R_{SC} + R_{SP}) = I_B R_S \quad (3)$$

where T_J is the junction temperature and R_S is the total series resistance. Because the avalanche breakdown voltage increases with increasing temperature and T_J increases because of Joule heating, the breakdown voltage, V_B , will increase with avalanche current, I_B , introducing another component of incremental resistance. This contribution to the small signal ac resistance of a diode in avalanche is the thermal resistance, R_{TH} , which is different from the heat flow resistance, θ , described in the previous section.

Haitz, Stover, and Tolar⁹ obtained values for thermal

⁹R. H. Haitz, H. L. Stover and N. J. Tolar, A Method for Heat Flow Resistance Measurements in Avalanche Diodes, *IEEE Trans. El. Dev. ED-16* (1969), 438.

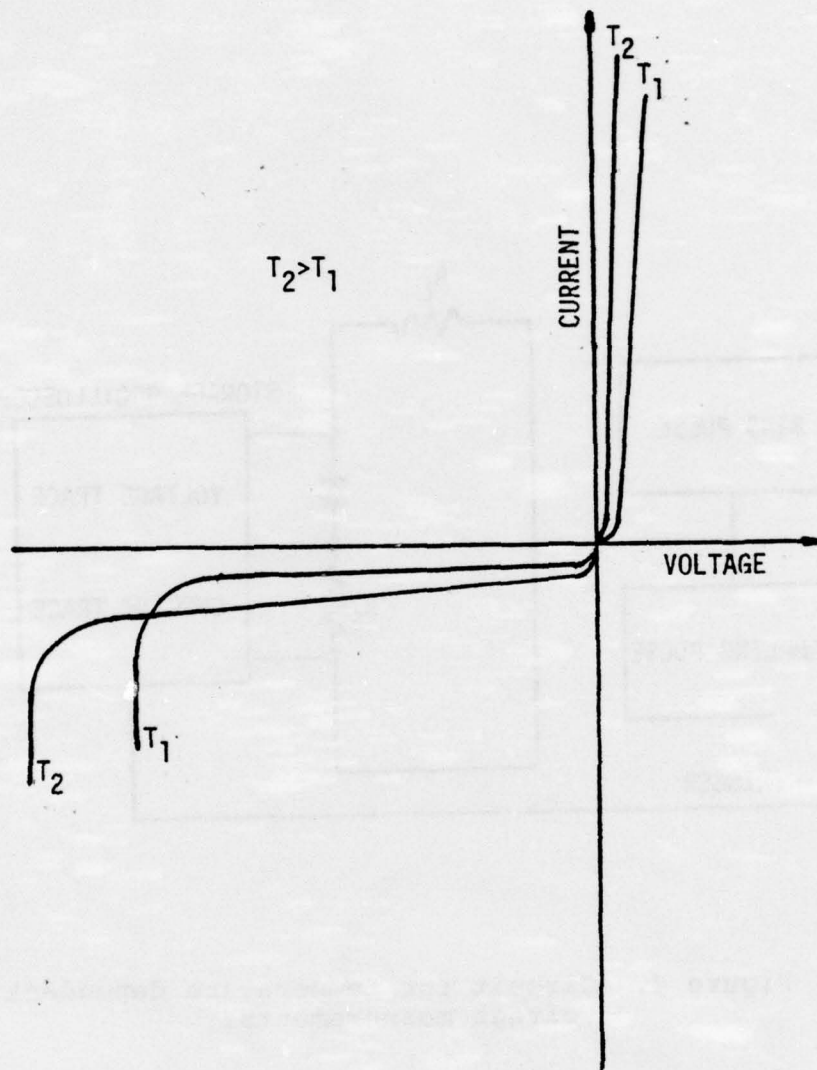


Figure 3. Effects of temperature on junction diode characteristics.

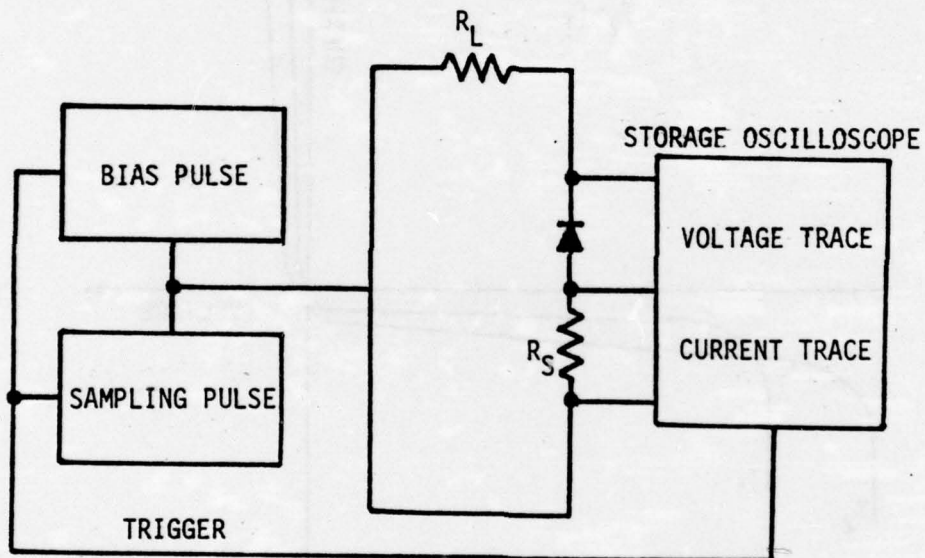


Figure 4. Circuit for temperature dependent voltage measurements.

and heat flow resistances by measuring the incremental ac resistance at various frequencies. At low frequencies, the junction temperature varies with the ac driving signal and a total resistance $R_{SC} + R_{SP} + R_{TH}$ is measured. At high frequencies, the junction temperature remains constant; with the thermal resistance absent, a resistance $R_S = R_{SP} + R_{SC}$ is measured.

Chiang and Lauritzen⁷ used these properties to determine the temperature of their diodes prior to second breakdown. If the temperature coefficient of avalanche breakdown voltage is $\Delta V_B / \Delta T$, then the breakdown voltage can be written as

$$V_B(T_J) = V_B(T_A) + \frac{\Delta V_B}{\Delta T} (T_J - T_A) \quad (4)$$

where T_A is the ambient or external case temperature. Eliminating $V_B(T_J)$ from Equations (3) and (4),

$$V - V_B(T_A) = I_B R_S + \frac{\Delta V_B}{\Delta T} (T_J - T_A) \quad (5)$$

If the breakdown voltage is measured at low currents to obtain $V_B(T_A)$, and the resistance R_S is obtained from a measurement of the high frequency ac incremental resistance, Equation (5) represents a steady-state procedure for obtaining the junction temperature T_J .

The transient method for measuring junction temperature does not require an explicit value for the resistance, R_S . When a fast risetime, constant current pulse is applied to a diode junction, the initial breakdown voltage occurs at $V_B(T_A)$. As the junction heats up, the voltage drop across it increases until the temperature reaches steady-state. If the pulse current is sufficiently high, the diode can be driven into second breakdown. The pulse length can be carefully controlled so that the voltage, hence the temperature, can be obtained before device damage occurs. Figure 6 shows the current and voltage waveforms for this technique. The junction temperature, T_J , can be obtained from the voltage difference

⁷K. L. Chiang and P. O. Lauritzen, *Thermal Instability in Very Small p-n Junction*, *IEEE Trans. El. Dev.*, ED-17 (1970), 782.

$$\begin{aligned}\Delta V(T) &= [V_B(T_J) + I_B R_S] - [V_B(T_A) + I_B R_S] \\ &= V_B(T_J) - V_B(T_A).\end{aligned}\quad (6)$$

But according to Equation (4),

$$V_B(T_J) - V_B(T_A) = \Delta V = \frac{\Delta V_B}{\Delta T} (T_J - T_A) \quad (4)$$

so that

$$T_J = \frac{\Delta V}{\Delta V_B / \Delta T} + T_A. \quad (7)$$

3. DIODE FABRICATION

Although small, flat junctions have been fabricated by diffusion⁷ for the purpose of obtaining single microplasmas, a different approach was employed in this work. The structure of silicon is such that, if alloying is performed into a (100) face, the alloyed region will be an inverted pyramid (figure 7). If aluminum is alloyed into n-type silicon, the resulting pyramidal alloyed structure is a p-n junction, with a high probability of microplasma formation at its apex.

Silicon dioxide layers 11000 Angstroms thick were grown at 1150°C in wet oxygen on 3 ohm-cm, n-type, (100) silicon substrates. Square window patterns, one edge aligned with the (110) direction, were etched through the oxide. An aluminum layer, 20000 Angstroms thick, was filament evaporated onto the substrate and through the windows in vacuum, and alloying was performed directly afterwards in vacuum, using a substrate heater.

In the initial stages of the work, the windows were .010 inch square, and alloying took place slightly above the eutectic temperature (577°C). Although the resulting device exhibited appropriate diode characteristics after the excess aluminum was removed in hydrochloric acid, con-

⁷K. L. Chiang and P. O. Lauritzen, *Thermal Instability in Very Small p-n Junction*, *IEEE Trans. EL. Dev.*, ED-17 (1970), 782.

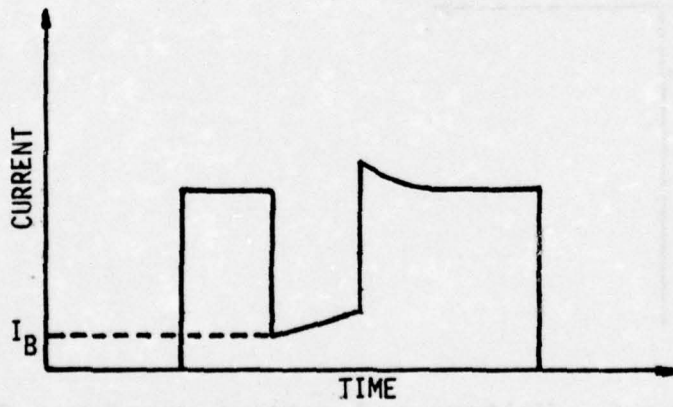
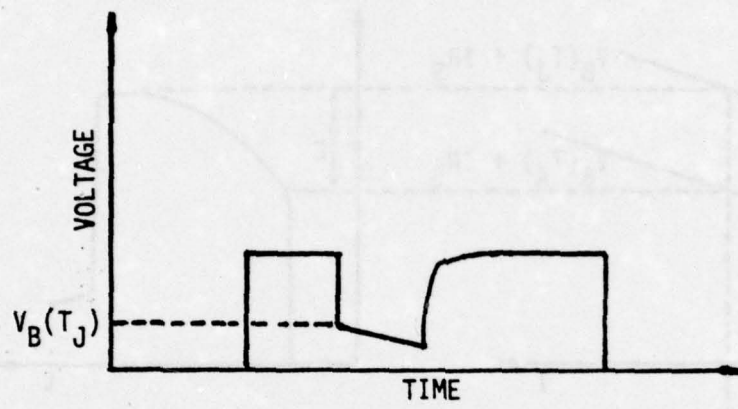


Figure 5. Voltage and current waveforms for the double-pulse measurement.

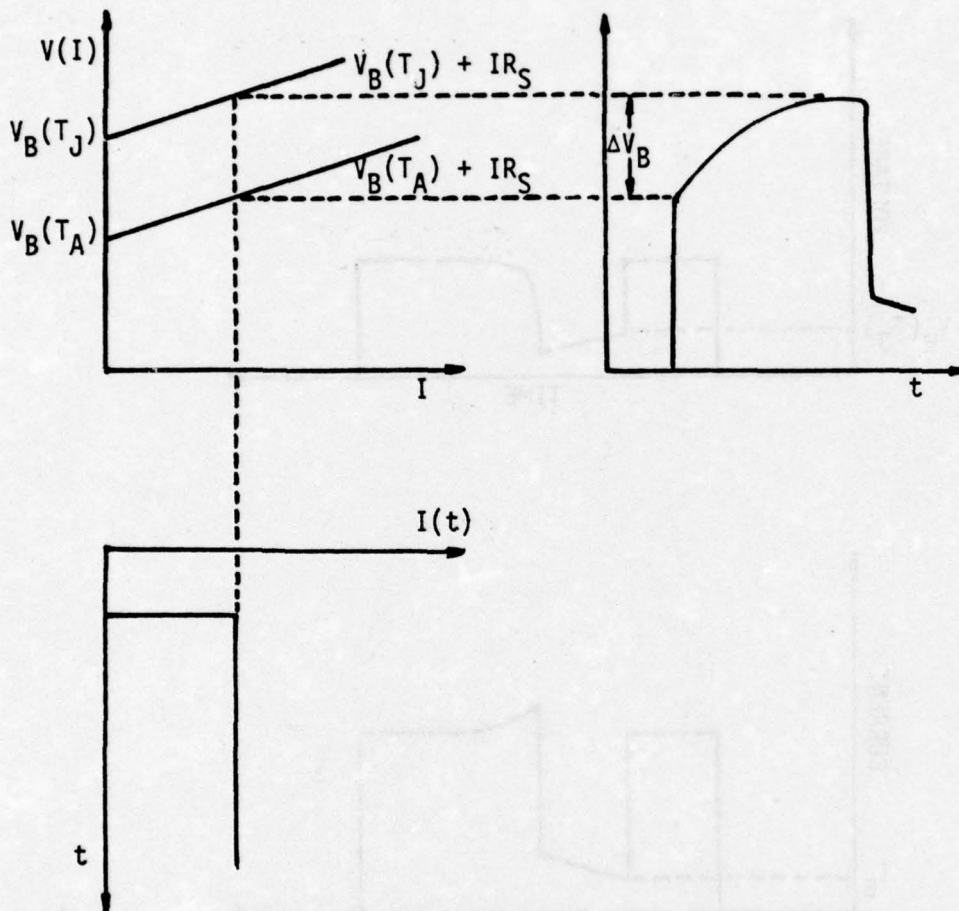


Figure 6. Voltage and current waveforms for the single-pulse measurement.

siderable non-uniformity was found to exist in the alloyed region. In fact, the region consisted of a number of scattered small square alloyed regions, around .001 inch on a side, all having the characteristic inverted pyramidal shape.

In order to obtain an optimum structure, a systematic study of window size effect on alloy uniformity was begun. Square windows, having dimensions of .001 inch to .008 inch on a side and aligned as before, were used in the formation of the junctions. Aluminum was evaporated over the entire substrate, but individual metal patterns were now etched, slightly overlapping the windows. The slices were sealed in quartz tubes under vacuum, and alloyed at temperatures between 557°C and 950°C, using various heating and cooling rates. It was found that, using this procedure, large pyramidal junctions could not be obtained; in fact, alloying was undesirably enhanced near the edge of the window, relative to the center. Also, the devices exhibited a soft avalanche knee, whereas a sharp breakdown was required for the temperature measurements.

After some additional experimentation without an oxide layer, it was found that diodes with the required characteristics could be obtained by evaporating the aluminum directly onto an unoxidized substrate, etching suitably aligned aluminum squares .001 inch on a side, and alloying around 700°C.

After alloying, the samples were dip-etched in a silicon clean-up etch. The diode characteristics directly after etching were not very good, but improved considerably after the devices aged in air for several days. Figure 8 illustrates the forward and reverse characteristics for a typical diode.

4. MEASUREMENTS AND RESULTS

Diodes were packaged in hybrid flat-packs using conductive epoxy adhesive, and the packages were placed in the sample holder; all leads were short, flat braid straps. Pulses were obtained from Hewlett-Packard Model 214-A pulse generators. In the double-pulse measurement, two were connected in tandem, one providing the bias pulse, the other, the sampling pulse, which could be delayed relative to the bias pulse. Only one pulse generator was

used in the single-pulse measurement. Current and voltage waveforms were displayed on a Tektronix 7633 storage oscilloscope. The current signals were fed into a wide-band plug-in amplifier; voltage waveforms were measured with a plug-in differential comparator. The use of the differential comparator was an improvement over previous measurements in two respects. First, the use of a wide-band, differential amplifier permitted the observation of the voltage across the diode directly, without calculation of the voltage drops across the series resistances in the diode loop. Second, it was now possible to float the waveform above zero, so that the important voltage fluctuations could be observed on a sensitive scale.

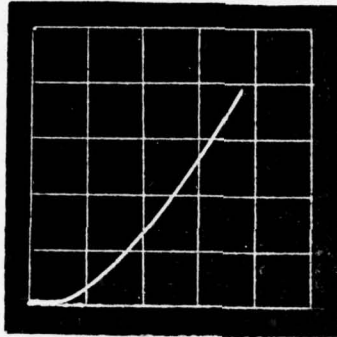
4.1 Temperature Coefficient of Avalanche Breakdown Voltage

The diode package was mounted in a teflon and aluminum probe assembly and placed in a Statham Model SD60 temperature test chamber. The steady-state junction temperature, that is, the temperature in the test chamber, was monitored with a chromel-alumel thermocouple. The reverse current defining the avalanche voltage was chosen to be 1 mA, primarily to assure that voltage fluctuations associated with the avalanche knee would not affect the measurements. The double-pulse technique was used, the bias pulse width selected to provide a reverse avalanche current twice that of the current defining avalanche. This current was reduced to 1 mA with the sampling pulse, so that the diode voltage at the leading edge of the sampling pulse was the avalanche breakdown voltage. The breakdown voltage was sampled in this manner at temperatures up to 260°C. The experimental values agreed with the theoretical prediction of a linear increase of breakdown voltage with increasing temperatures.⁷

4.2 Junction Temperature at Second Breakdown

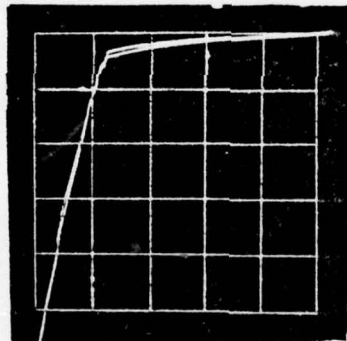
At first, when the double pulse technique was used, the biasing pulse drove the device into second breakdown so quickly, that it was not possible to introduce the sampling pulse. The limiting resistance, R_L , in the cir-

⁷ K. L. Chiang and P. O. Lauritzen, *Thermal Instability in Very Small p-n Junction*, *IEEE Trans. El. Dev.*, ED-17 (1970), 782.



a. Forward current *vs.* forward bias voltage.

Vertical Scale: 10 μA per division.
Horizontal Scale: 0.5 V per division.



b. Reverse current *vs.* reverse bias voltage.

Vertical Scale: 100 μA per division.
Horizontal Scale: 5 V per division.

Figure 8. Measured diode characteristic curves.

cuit of figure 4 was increased, reducing the current and increasing the delay time to a value large enough to accommodate the sampling pulse. Bias pulse widths were limited to 60 μ s to prevent junction damage in second breakdown; total power dissipated by the device was not permitted to exceed that value used in the determination of the heat flow resistance. However, the sampling pulse introduced perturbations which made it difficult to determine precisely the power level at its leading edge.

In the single-pulse measurements, R_L was made very large to provide nearly constant current. Inasmuch as the power applied to the junction is small in this measurement, longer pulses were required to input the same energy as in the double-pulse method. Figure 9a shows a typical junction voltage waveform when the constant current pulse is applied. The direction of increasing current is upwards; however, voltage is shown increasing downwards because of the voltage floating on the comparator. This is consistent with increasing reverse voltage drop. According to this convention, the device is hard into second breakdown late in the pulse., when the reverse voltage drop is small. During the actual measurement, the pulse length was reduced (figure 9b).

The results of both the double and single-pulse measurements are shown in table I. The junction temperatures have been corrected to take account of junction heating; the values of heat flow resistance used in the corrections were obtained near the measured temperature.

5. DISCUSSION OF RESULTS

According to recent work,^{3,5,6} second breakdown can be divided into three stages: nucleation, growth, and melt. Nucleation, which is followed by heating and cur-

³P. P. Budenstein, D. H. Pontius and W. B. Smith, *Second Breakdown Damage in Semiconductor Junction Devices*, US Army Missile Command, Redstone Arsenal, Report RA-TR-72-15 (1972).

⁵R. Sunshine, *Avalanching and Second Breakdown in Silicon-on-Sapphire Diodes*, Ph.D. Dissertation, Princeton University (1971).

⁶W. B. Smith, D. H. Pontius and P. P. Budenstein, *Second Breakdown and Damage in Junction Devices*, *IEEE Trans. El. Dev.*, ED-20 (1973), 731.

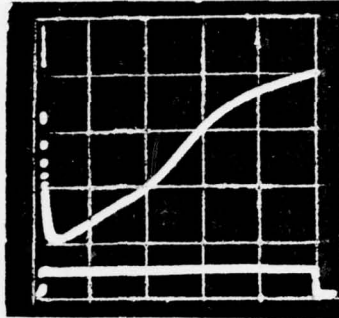
rent channelling, occurs when the local temperature in the junction reaches a critical value. Constant current pulsing produces only a very slight reduction in the voltage drop across the device during nucleation; nucleation also does not degrade device characteristics or damage the device. If the pulse is of sufficient amplitude and duration, the channeled current, or filament, spreads into the high resistance region adjacent to the junction. This is accompanied by a larger voltage drop, but device damage still does not result. The most significant drop in voltage occurs when the local temperature exceeds the peak of the temperature-resistivity curve, following which the current filament spreads completely through the high resistivity region, and a melt channel forms, accompanied by a rapid localized increase in temperature. Reverse characteristics are irreversibly affected at this time. These stages are illustrated in figure 10, which represents a typical waveform obtained in that work.

Figure 11 shows a slight dip in the voltage drop across the junction; this dip occurred in all the measurements. The dip is well defined and appears shortly after the application of the current pulse. Although somewhat different from similar dips associated with nucleation,³ which were subtle fluctuations taking place later in the pulse, the dip probably signals the onset of nucleation in these measurements.

The acuteness of the dip is consistent with the existence of only one nucleation center, the apex of the pyramidal junction. A single nucleation center is also consistent with the rapid transition into second breakdown exhibited by the test devices (figure 9b). If the current is constrained to flow in a single channel, early second breakdown is accelerated through the formation of a single hot-spot.

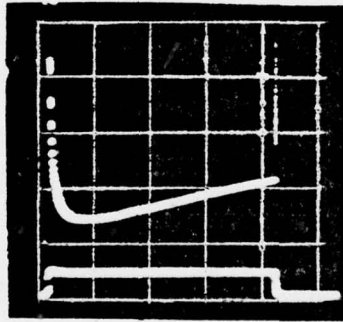
Nucleation occurs when the sum of the minority and thermally generated carrier current densities equals the current density of the applied pulse. Broad filamentation does not take place until the local temperature becomes greater than the peak of the resistivity-temperature

³P. P. Budenstein, D. H. Pontius and W. B. Smith, *Second Breakdown Damage in Semiconductor Junction Devices*, US Army Missile Command, Redstone Arsenal, Report RA-TR-72-15 (1972).



a. Long current pulse

Upper Curve: Junction reverse voltage *vs.* time.
 Vertical Scale: 2 V per division increasing downward.
 Horizontal Scale: 50 μ s per division.
 Lower Curve: Input current *vs.* time.
 Vertical Scale: 20 mA per division.
 Horizontal Scale: 50 μ s per division.



b. Short current pulse

Upper Curve: Junction reverse voltage *vs.* time.
 Vertical Scale: 1 V per division increasing downward.
 Horizontal Scale: 10 μ s per division.
 Lower Curve: Input current *vs.* time.
 Vertical Scale: 20 mA per division.
 Horizontal Scale: 10 μ s per division.

Figure 9. Junction reverse voltage waveforms with constant current pulses.

TABLE I. SUMMARY OF TEMPERATURE MEASUREMENTS

Device No.	V_B^1 (volts)	$\frac{\text{Double-Pulse}^2}{\theta}$ (°C/watt)	T_J^2 (°C)	$\frac{\text{Single-Pulse}^3}{T_J}$ (°C)
1	43	21	225	225
2	43	25	265	245
3	50	21	225	245
4	46	21	225	245
5	46	21	225	255
6	43	21	225	245

¹Ambient temperature: 25°C; I_B : 1 milliampere

²Input power: 4.8 watts

³Input power: 2.3 watts

curve (figure 12) corresponding to the resistivity of the lightly-doped side of the junction. The current is no longer ballasted by the positive temperature coefficient of resistance, and thermal runaway takes place, followed by damage or even local melting. For a substrate resistivity of 3 ohm-cm, the peak occurs at around 210°C. This value is in satisfactory agreement with the average measured junction temperature, 232°C by the double-pulse technique, and 243°C by the single-pulse technique.

In summary, the experimental evidence supports the existence of a single microplasma at the apex of a pyramidal junction. The junction temperatures measured just before second breakdown by two different pulse techniques are in good agreement with each other, and support a thermal runaway mechanism.

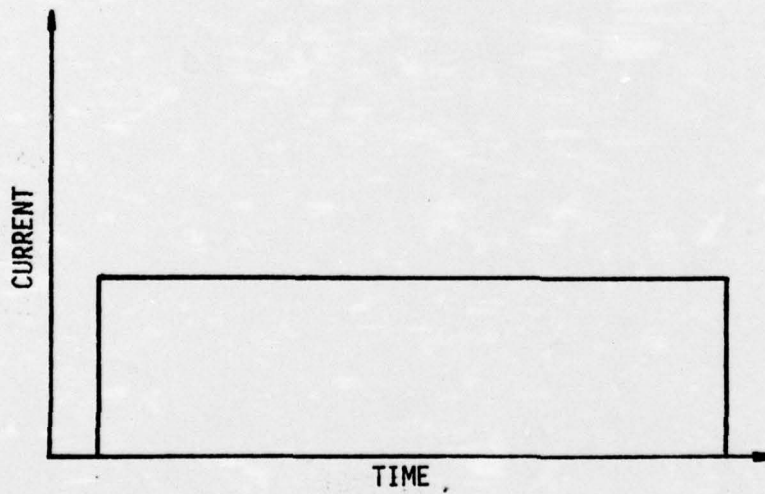
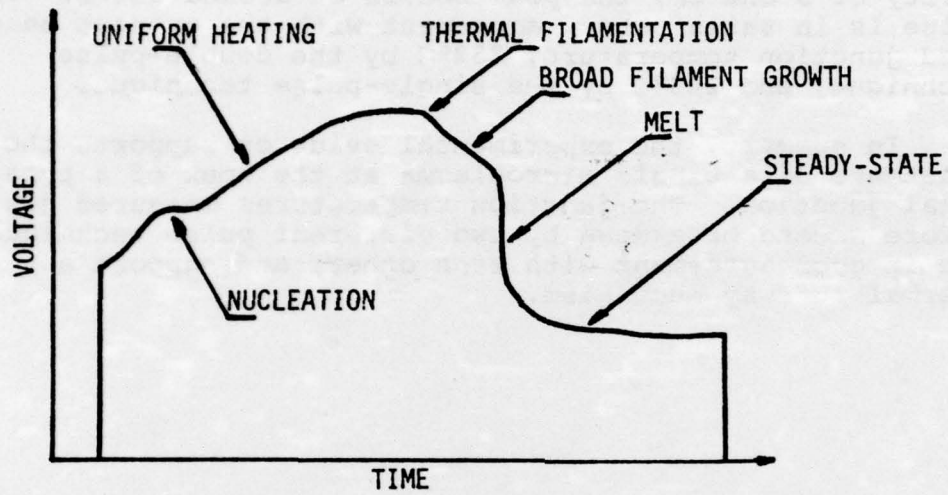
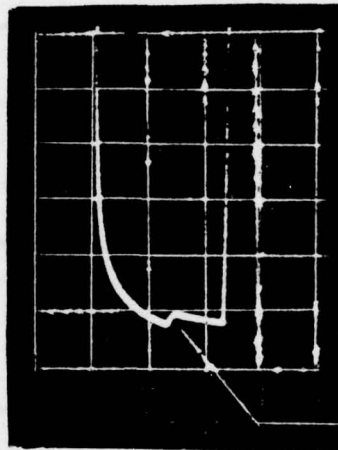


Figure 10. Events in second breakdown: junction reverse voltage with a constant current pulse.



Vertical Scale: 2 V per division increasing downward.
Horizontal Scale: 1 μ s per division.

Figure 11. Junction reverse voltage vs. time: current nucleation.

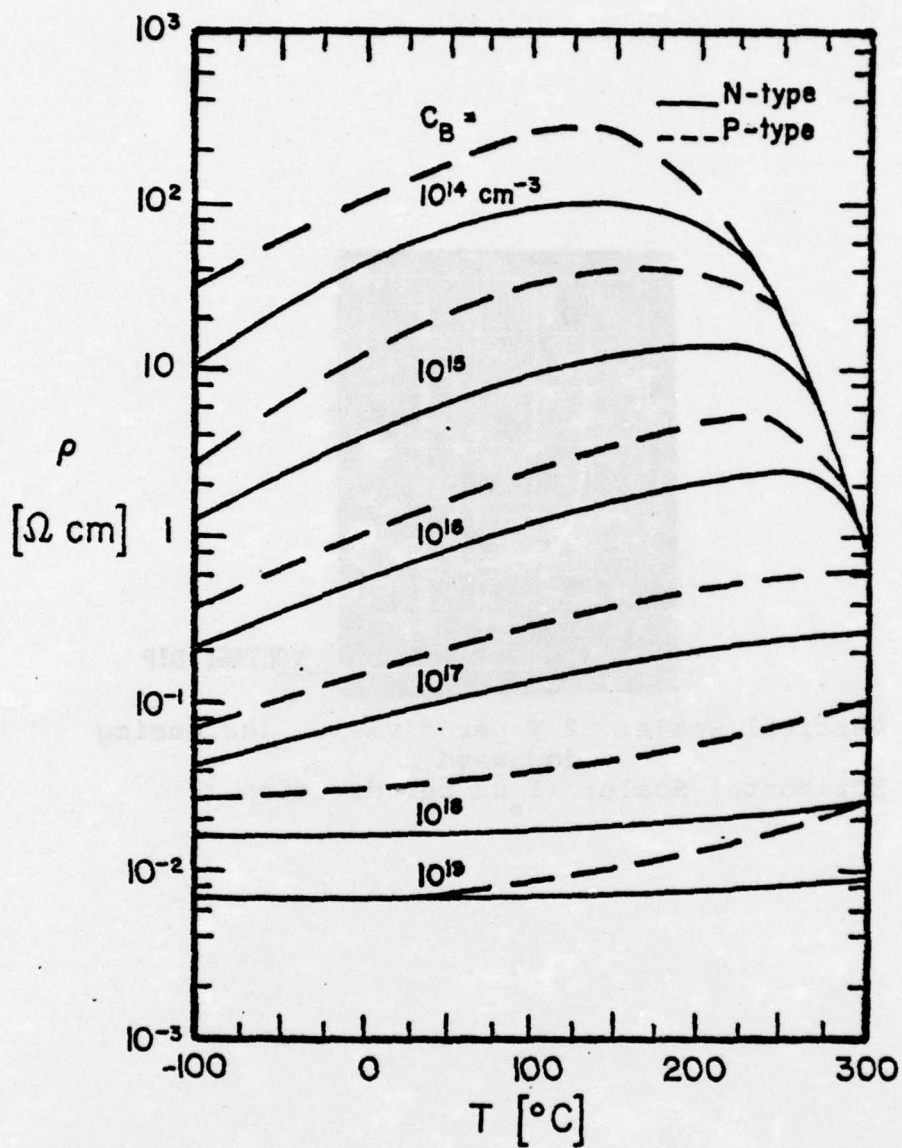


Figure 12. Resistivity-temperature curves for silicon (excerpt from Silicon Semiconductor Data, H. F. Wolf, Pergamon Press, New York (1969), 51).

6. LITERATURE CITED

- (1) H. A. Schaft, Second Breakdown - A Comprehensive Review, Proc. IEEE, 55 (1967), 1272.
- (2) H. Potash and W. W. Happ, Modeling Procedures for Interactions Between Thermal and Electrical Device Parameters, Solid-St. Electr., 10 (1967), 737.
- (3) P. P. Budenstein, D. H. Pontius and W. B. Smith, Second Breakdown Damage in Semiconductor Junction Devices, US Army Missile Command, Redstone Arsenal, Report RA-TR-72-15 (1972).
- (4) P. P. Budenstein, A Survey of Second Breakdown Phenomena, Mechanisms, and Damage in Semiconductor Devices, Defense Documentation Center Report AD-721294 (1970).
- (5) R. Sunshine, Avalanching and Second Breakdown in Silicon-on-Sapphire Diodes, Ph.D. Dissertation, Princeton University (1971).
- (6) W. B. Smith, D. H. Pontius and P. P. Budenstein, Second Breakdown and Damage in Junction Devices, IEEE Trans. El. Dev., ED-20 (1973), 731.
- (7) K. L. Chiang and P. O. Lauritzen, Thermal Instability in Very Small p-n Junction, IEEE Trans. El. Dev., ED-17 (1970), 782.
- (8) J. Nigrin, Pulse Measurements of Transient Thermal Response and Temperature of Avalanching p-n Junction, Electr. Letters, 1 (1971), 481.
- (9) R. H. Haitz, H. L. Stover and N. J. Tolar, A Method for Heat Flow Resistance Measurements in Avalanche Diodes, IEEE Trans. El. Dev. ED-16 (1969), 438.
- (10) H. F. Wolf, Silicon Semiconductor Data, Pergamon Press, New York (1969), 51.

7. SELECTED BIBLIOGRAPHY

Alibjian, R. K., Effect of Wafer Thickness Upon the Breakdown Voltage of Silicon Diodes, Solid-St. Electr., 11 (1968), 574.

Azarewicz, J. L., Transient Radiation Effect Research, U.S. Army Materials Command, Report HDL-TR-060-2 (1973).

Browne, V. A., Lewis, D. G. and Mars, P., Measurement of p-n Junction Second Breakdown Characteristics, Int. J. Electr. 31 (1971), 127.

Chen, H. C., Portnoy, W. M. and Ferry, D. K., Doping Dependence of Second Breakdown in a p-n Junction, Solid-St. Electr., 14 (1971), 747.

Cohn, N. S., Susceptibility of Semiconductor Devices to Thermal Second Breakdown, Naval Ordnance Laboratories Report SHIP-17095/54814 (1973).

Cohn, N. S., Susceptibility of Semiconductor Devices to Thermal Second Breakdown, 12th Annual International Reliability Physics Symposium, Las Vegas, Nevada (1974).

Cohn, N. S. and Petree, M. C., Second Breakdown in Germanium Gold Bonded Diodes, Laboratories Report NOL-TR-72-56 (1972).

Dumin, D. J., Emission of Visible Radiation from Extended Plasmas in Silicon Diodes During Second Breakdown, IEEE Trans. El. Dev., ED-16 (1969), 479.

Dostoomian, A. S. and Nowakowski, M. F., IR Analysis of Second Breakdown Modes in Power Transistors, IEEE International Convention Digest, (1968), 97.

Elsharkawi, A. R. and Kao, K. C., Effects of Temperature on Current Instabilities Caused by Recombination Centers in Semiconductors, Solid-St. Electr., 16 (1973), 1355.

Fabricius, E. D., The Mechanism of Second Breakdown in Transistors, Ph.D. Dissertation, Newark College of Engineering (1968).

Fleming, D. J., Thermal Breakdown Delay Time in Silicon p-n Junctions, IEEE Trans. El. Dev. ED-18 (1971), 94.

Gaur, S. P., Transistor Design and Thermal Stability, IEEE Trans. El. Dev. ED-20 (1973).

Gibbons, G. and Misawa, T., Temperature and Current Distributions in an Avalanching p-n Junction, Solid-St. Electr., 11 (1968), 1007.

Hower, P. L. and Govil, P. K., Comparison of One and Two-Dimensional Models of Transistor Thermal Instability, IEEE Trans. El. Dev. ED-21 (1974), 617.

Kalab, B., Analysis of Failure of Electronic Circuits from EMP-Induced Signals, U.S. Army Material Command Report HDL-TR-1615 (1973).

Kazakevich, V. I., The Effect of Electron Bombardment on Second Breakdown in Transistors, Army Electronics Command (1970).

Krishna, S. and Hower, R. L., Second Breakdown of Transistors During Inductive Turnoff, Proc. IEEE (1973), 393.

Lugue, A. and Dehasa, C., Two Piece Model of Hot Point Generation in Reverse Biased p-n Diodes, Solid-St. Electr., 17 (1974), 165.

Mahadevan, S., Hardas, S. M. and Suryan, G., Electrical Breakdown in Semiconductors, Solid State Physics. 8 (1971), 335.

Mars, P., Thermal Analysis of p-n Junction Second Breakdown Initiation, Int. J. Elect. 33 (1971), 596.

Nakahara, O., Effects of Collector Structures on Reverse Bias Second Breakdown of Transistors, Proc. IEEE, (1968), 123.

Navon, D. A., Power Transistor Stability and Reliability, Defense Documentation Center Report AD-751852 (1972).

Navon, D. and Miller, E. A., Thermal Instability in Power Transistor Structures, Solid-St. Electr., 12 (1969), 69.

Nelson, D. L., Sweet, R. J. and Niehaus, D. J., Study to Investigate the Effects of Ionizing Radiation on Transistor Surfaces, NASA Report NAS 8-20135 (1967).

Pontius, D. H., Effect of Ionizing Radiation on Second Breakdown, Solid-St. Electr., 16 (1973), 1073.

Poorter, T., The Relation Between Reverse Secondary Breakdown Behavior and the Properties of Planar Epitaxial Power Transistors, Philips Research Reports, 23 (1968), 281.

Popescu, C., Self Heating and Thermal Runaway Phenomena in Semiconductor Devices, Solid-St. Electr., 13 (1970), 441.

Popescu, C., Thermal Runaway Mechanism of Second Breakdown Phenomena, Solid-St. Electr., 13 (1970), 887.

Popescu, C., The Second Breakdown in Reverse Biased Transistor as an Electrothermal Switching, IEEE Trans. El. Dev., ED-21 (1974), 428.

Raburn, W. D., The Determination of Semiconductor Junction Vulnerability to Second Breakdown by Low Energy Electrical Measurements, Final Report, U.S. Army Missile Command, Redstone Arsenal (1973).

Reich, B., Effects of Neutron Radiation on Second Breakdown and Thermal Behavior of Silicon Transistors, U.S. Army Electronics Command, Report ECOM-3098 (1969).

Reich, B., Hot Spot Thermal Resistance in Transistors, IEEE Trans. El. Dev., ED-16 (1969), 166.

Reich, B., RF Power Transistors for Reliable Communication Systems, IEEE Trans. El. Dev. (1970), 816.

Roman, G., A Model for Computation of Second Breakdown in Transistors, Solid-St. Electr., 13 (1969), 961.

Schench, J. and Midford, T., Failure Modes in Silicon Avalanche Transit Time Microwave Devices, IEEE Trans. El. Dev., ED-14 (1967), 619.

Shapovalov, V. P., The Formation of Secondary Breakdown in Germanium p-n Junctions IEEE Trans. El. Dev. ED-18 (1971), 501.

Speeney, D. V. and Carey, G. P., Experimental Study of the Effect of Junction Curvature on Breakdown Voltage in Silicon, Solid-St. Electr., 10 (1967), 177.

Spitzer, S. M., Thermal Instabilities Limiting Power Dissipation in Transistors, Solid-St. Electr., 12 (1969), 433.

Thompson, I. and Wilkerson, E., Destructive Reverse Breakdown in Large Area Phosphorous Diffused High Voltage Silicon n + p Junctions, Solid-St. Electr., 10 (1967), 938.

Tyagi, M. S., Zener and Avalanche Breakdown in Silicon Alloyed p-n Junctions, Solid St. Electr., 11 (1968), 99.

Wang, C., Temperature Effects in Semiconductor Avalanches, Ph.D. Dissertation, Cornell University (1970).

Wang, P. P., Thermal Instability and Secondary Breakdown in Power Transistors, IEEE Trans. Aerosp. and El. Syst. AES-7 (1971), 1195.

Wilson, H. B., Feasibility of Using Finite Elements in Analysis of Second Breakdown in Semiconductor Device, Defense Documentation Center Report AD-766688 (1973).

8. DISTRIBUTION

<u>Department of Defense</u>	<u>No. of Copies</u>
Defense Documentation Center Cameron Station, Building 5 Alexandria, Va. 22314 ATTN: DDC-TCA	8
Director Defense Advanced Rsch Proj. Agency Architect Building 1400 Wilson Blvd. Arlington, VA. 22209 ATTN: Technical Library	1
Director Defense Civil Preparedness Agency Assistant Director for Research Washington, D. C. 20301 ATTN: Admin. Officer	1
Defense Communication Engineer Center 1860 Wiehle Avenue Reston, Va. 22090 ATTN: CODE R720, C. Stansberry	1
Director Defense Nuclear Agency Washington, D. C. 20305 ATTN: DDST ATTN: RAEV ATTN: STTL Tech Library	1 1 1
Director of Defense Research and Engineering Department of Defense Washington, D.C. 20301 ATTN: DD/S&SS	1
Director National Security Agency Ft. George G. Meade, Md. 20755 ATTN: Technical Library	1

<u>DEPARTMENT OF THE ARMY</u>	<u>No. of Copies</u>
Commander US Army Material Development & Readiness Command 5001 Eisenhower Avenue Alexandria, Va. 22333 ATTN: DRXAM-TL, HQ Tech Library	1
Commander US Army Electronics Command Fort Monmouth, N.J. 07703 ATTN: DRSEL-TL-IR, Robert A. Freiberg ATTN: DRSEL-TL-MD, Gerhart K. Gaule	1 1
Commander US Army Missile Command Redstone Arsenal, Ala. 35809 ATTN: Technical Library	1
Commander US Army Mobility Equipment R&D Center Fort Belvoir, Va. 22060 ATTN: Technical Library	1
Commander US Army Nuclear Agency Fort Bliss, TX. 79916 ATTN: Technical Library	1
 <u>DEPARTMENT OF THE NAVY</u>	
Chief of Naval Research Department of the Navy Arlington, VA. 22217 ATTN: Technical Library	1
Commander Naval Electronic Systems Command Headquarters Washington, D.C. 20360 ATTN: Technical Library	1
Commander Naval Surface Weapons Center White Oak, Silver Spring, MD. 20910 ATTN: Code WX21, Tech Lib	1

DEPARTMENT OF THE AIR FORCE

NO. OF
Copies

Air Force Weapons Laboratory, AFSC
Kirtland AFB, N.M. 87117
ATTN: EL, Mr. John Darrah
ATTN: DYX, Donald C. Wunsch
ATTN: ELP, Carl E. Baum

1
1
1

UNIVERSITY

Auburn University
Physics Department
Auburn, Alabama 36830
ATTN: Dr. P. P. Budenstein

1

Harry Diamond Laboratories

Commander
Harry Diamond Laboratories
2800 Powder Mill Road
Adelphi, Maryland 20783

ATTN: DRXDO-TC, I. N. Flyer (Actg) 1
DRXDO-TB, P. E. Landis (Actg) 1
DRXDO-TE, Dr. H. Sommer 1
DRXDO-TF, Dr. R. B. Oswald (Actg) 1
DRXDO-TD, Dr. W. W. Carter 1
DRXDO-TD, S. M. Marcus (Tech Assist.) 1
DRXDO-NP, F. M. Wimenitz 1
DRXDO-RB, R. J. Bostak 1
DRXDO-RD, Q. C. Kaiser 1
DRXDO-EM, R. E. McCoskey 1
DRXDO-EM, R. Pfeffer 1
DRXDO-EM, G. Gornak 1
DRXDO-EM, J. Dando 1
DRXDO-EM, J. Kreck 4
DRXDO-TI, 010 3
DRXDO-TI, 013 1